Proceedings of BS2013:
13th Conference of International Building Performance Simulation Association, Chambéry, France, August 26-28

EXPERIMENTS ON INVERSE METHOD TO ILLUMINATION BY OPTIMIZATION TECHNIQUE - IMIBYOPTIM

Letícia Jenisch Rodrigues[1,2], Paulo Smith Schneider[2], Tiago Haubert Andriotty[2], and Francis Henrique Ramos França[2]
[1]Instituto Federal de Educação Ciência e Tecnologia do Rio Grande do Sul Campus Farroupilha. Av. São Vicente, 785, 95180-00, Farroupilha, RS, Brazil
[2]Universidade Federal do Rio Grande do Sul, Escola de Engenharia, Depto. de Eng. Mecânica. Rua Sarmento Leite, 425, Centro Histórico, 90050-170, Porto Alegre, RS, Brazil.

ABSTRACT

The present work reports an experimental procedure designed to verify a particular solution for the distribution of artificial light sources. The inverse method to illumination by optimization technique, *IMIbyOPTIM*, is applied to generate an uniform field of illumination as a result of the free location of purely diffuse light sources. A reduced scale enclosure is build to measure the effectiveness of the method on indoor environments. The illumination field is observed over a work plane placed parallel to the floor and measured by photovoltaic sensors. The results measured on the workbench are similar to the simulation case, since the overall average shows that the mean value is close to the unitary target, with a standard deviation less then 0.0065. The largest relative difference between the results was 3.58%, while the lowest was 0.03%.

INTRODUCTION

The design of lighting systems for indoor spaces aims to find a solution that provides a uniform illumination over a selected surface, called the work plane. This uniformity provides adequate working conditions, avoiding uncomfortable postures and contributes to the mitigation of visual discomfort, known as reddened eyes. Its application is not limited to human ergonomic factors, as reported by (Jordan and Tavares, 2005), who present experiments on aviaries associating the increase on animal production related to parameters of the lighting system. Similar effect was described by (Cavichioli et al., 2006) on the growth of plant species, due to well adjusted lighting intensity and distribution. The early methods for the analysis and design of artificial lighting of environments appeared in the beginning of the 20th century. It was already known that the luminous flux on a given incident plan was not only dependent on the light sources power, but also on the absorbing and reflecting effect over the enclosure surfaces.

The first work to deal with illumination design was presented by Harrison and Anderson (1916, 1920), who proposed an experimental procedure that is known nowadays as the Lumen method, in which the luminous flux on a given work plane was determined from the combination of punctual and continuous light sources. In the forties, Moon (1941) and Moon and Spencer (1946b,a) proposed the interreflection method for the design of three-dimensional rectangular enclosures with purely diffuse surfaces of any aspect ratio. The method presented the advantage of allowing the calculation of the brightness of a surface, accounting for the reflection of light. A solid contribution to the illumination analysis arose from the advances in the understanding of thermal radiation exchanges by Hottel and Sarofim (1967); Siegel and Howell (2002). In the second half of the 20th century, as light from incandescent lamps or bulbs is actually thermal radiation in the visible region of the spectrum. Therefore, the analytical and computational methods developed for the solution of thermal radiation problems in enclosures could be readily extended for the illumination, as the thermal radiation flux can be converted into the luminous flux, accounting for the photopic luminous efficacy of the human eye.

The Lumen method (IESNA, 2000), as well as the point-to point method (EEE/SA, 2012) starts from a given scenario, proposed by the designer, and ends up on a spacial distribution of the lighting sources and auxiliary assembling (the lighting system) on the seeling. Both methods are based on trail and error, forcing the designer to specify the placement and power of the light sources, and to run a computational routine to find the resulting illuminance on the work plane. If the solution is not the expected one, calculation must be redone until a satisfactory solution is achieved. Due to the complexity of the light transport, it is in general very difficult to make a new guess from a previous attempt. The designer is left to choose the best solution from a collection of trials, which is probably not the best possible one.

In this context, the inverse method arises as a promising option. It consists of defining the value of the lighting in the work plan as one of the boundary conditions of the problem. The unknown variables are the positions and intensities of the light sources, whose values are determined by the method. A first attempt was proposed by (Fontana et al., 2004), which solution generated ill-conditioned equations systems, which required a regularization method (TSVD) to be solved. This approach was later explored by (Seewald, 2006), for a more detailed spectral behavior of the lightning sources and surface response. The same authors com-

pared computational results from the method of Lumens to the ones obtained out of the inverse method, which were again used in later works (Schneider and França, 2008; Schneider et al., 2009). A comprehensive review of inverse design involving radiative exchanges in enclosures is presented in (França et al., 2002).

As a new step to solve the problem by first satisfying the illuminance uniformity over the work plane, (Cassol, 2009) applied an optimization procedure to replace the TSVD method. This optimization algorithm, called Generalized Extremal Optimization-GEO (de Sousa et al., 2003), is a stochastic method based on random search, guided by probabilistic decisions, which aims to find a global minimum or a maximum, depending on the case. The application of this method yielded satisfactory results, with maximum deviations close to those found by (Seewald, 2006), confirming the correctness of the inverse methodology. Based on these observations, the approach was called the Inverse Method to Illumination by Optimization Technique (*IMIbyOPTIM*), which is a new methodology to find the location and the luminous power of the light sources to satisfy a prescribed illuminance over the work plane with the constraint of lowest power consumption.

In this context, the present work aims to experimentally evaluate the validity of results generated by the (*IMIbyOPTIM*). A reduced scale indoor workbench was built to verify the illuminance in the work plane created by a particular configuration of lamps and the quality of the uniformity produced by the inverse method.

THE IMIbyOPTIM METHOD

A schematic representation of the system is shown in Figure 1.

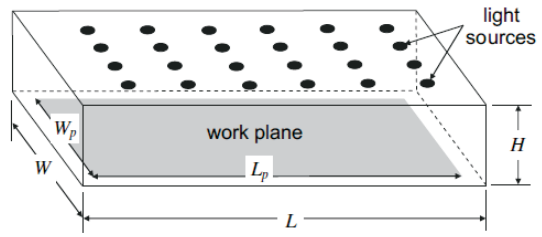

Figure 1: The generic illumination system with uniform light source distribution on the ceiling.

The three-dimensional rectangular enclosure is formed by surfaces that are perfectly diffuse. The work plane, where the incident illuminance is to be specified, is located on the bottom surface of the enclosure; the light sources are located on the top surface. The remaining of the enclosure is formed by walls that partially reflect incident light. The length, width and height of the enclosure are designated by L, W and H, respectively. Due to the physical symmetry of the examples considered in this paper, only one-quarter of the system needs to be solved. The enclosure is divided into finite-sized square elements, $\Delta x = \Delta y = \Delta z$, in which the luminous energy balance will be applied. The work plane, light sources and walls elements are designated by kp, kl and kw, respectively. The number of elements on the work plane, light sources and walls in the one-quarter of the system are designated by KP, KL and KW, so $1 \leq kp \leq$ KP, $1 \leq kl \leq$ KL and $1 \leq kw \leq$ KW. When a general relation applies to any kind of surface element, the general index k will be used.

Theoretical Modelling

An uniform illuminance, indicated by $L_{i,specified}$ (in units of lumens/m^2 or lux), is specified on the work plane. The design problem consists of finding the location and power of the light sources to attain the specified illuminance. The incident illuminance on element kp in the work plane, $L_{i,kp}$, in lux, is a result of multiple reflections of the light in all surfaces, and can be computed from:

$$L_{i,kp} = \left(\sum_{kp^*=1}^{KP} F_{kp-kp^*} L_{0,kp^*} + \sum_{kl=1}^{KL} F_{kp-kl} L_{0,kl} + \sum_{kw=1}^{KW} F_{kp-kw} L_{0,kw} \right) \quad (1)$$

where $L_{0,k}$ (in lux) is the outgoing illuminance or luminous radiosity of surface element k, which takes into account both emission and reflection, and F is the view factor between surface elements k and $k*$. When elements k and $k*$ are on the same plane, the respective view factor will be equal to $zero$, as with the work plane elements in Figure 1. In spite of this, all view factors are being kept in the formulation to accommodate the cases in which the elements are not in the same plane.

For a more general presentation of the solution, all results in this paper are presented in dimensionless form. The dimensionless incident illuminance on each work plane element is

$$l_{i,kp} = \frac{L_{i,kp}}{L_{i,spf}} \quad (2)$$

so the target of the work plane is that $l_{i,kp}$ be as close as possible of the unit. Equation 1 can be expressed in dimensionless form by:

$$l_{i,kp} = \left(\sum_{kp^*=1}^{KP} F_{kp-kp^*} l_{0,kp^*} + \sum_{kl=1}^{KL} F_{kp-kl} l_{0,kl} + \sum_{kw=1}^{KW} F_{kp-kw} l_{0,kw} \right) \quad (3)$$

where

$$l_{0,kp} = \frac{L_{0,kp}}{L_{i,spf}} \quad (4)$$

is the dimensionless outgoing illuminance of surface element k. According to Equation 3, to determine the incident illuminance on the work plane, it is first necessary to determine the dimensionless outgoing illuminance of all surface elements, which are given by the following relations:

$$l_{0,kp} = \rho_{kp}\left(\sum_{kp*=1}^{KP} F_{kp-kp*} l_{0,kp*} + \sum_{kl=1}^{KL} F_{kp-kl} l_{0,kl} + \sum_{kw=1}^{KW} F_{kp-kw} l_{0,kw}\right) \quad (5)$$

$$l_{0,kl} = e_{kl} + \rho_{kl}\left(\sum_{kp=1}^{KP} F_{kl-kp} l_{0,kp} + \sum_{kl*=1}^{KL} F_{kl-kl*} l_{0,kl*} + \sum_{kw=1}^{KW} F_{kl-kw} l_{0,kw}\right) \quad (6)$$

$$l_{0,kw} = \rho_{kw}\left(\sum_{kp=1}^{KP} F_{kw-kp} l_{0,kp} + \sum_{kl=1}^{KL} F_{kw-kl} l_{0,kl} + \sum_{kw*=1}^{KW} F_{kw-kw*} l_{0,kw*}\right) \quad (7)$$

In the above equations, ρ_{kw} is the hemispherical reflectivity of surface element k in the visible range of the spectrum. The dimensionless luminous power of the light source element kl is defined as

$$e_{kl} = \frac{E_{kl}}{L_{i,spf}} \quad (8)$$

where E_{kl} (in lux) is its luminous power. As described by Equations 5 to 7, the outgoing illuminance of the work plane and wall elements correspond solely to the reflection of the incident illuminance; no light is emitted from the work plane and wall elements, so the luminous power is null for those elements (e_{kp} = e_{kw} = 0). For the light sources elements, outgoing illuminance is the sum of the luminous power and the reflection of the incident illuminance.

In the conventional forward design of illumination systems, the dimensionless power and location of each light source element, e_{kl}, is prescribed. It follows that Equations 5 to 7 form a system of linear equations on the outgoing illuminance of all surface elements. The system presents the same numbers of equations (i.e., one equation for each element) and of unknowns (i.e., the outgoing illuminance of each element), and can be solved by any standard matrix solver, such as Gauss-Seidel and Gaussian elimination. After the solution of the $l_{0,k}$s, Equation 3 is applied to each work plane element kp to determine its dimensionless illuminance, $l_{i,kp}$, which is then compared to the desired value, $l_{i,spf}$. The drawback of this approach is that choosing the location and luminous power of the light sources to lead to the specified illuminance on the work plane is very difficult. In the conventional approach, a number of solutions are tried, and then the best attempt of the set is selected. However, the selected solution will probably not be the best possible solution.

The inverse design methodology described in França et al. (2002); Ertürk et al. (2002); França and Howell (2006); Daun et al. (2006); Schneider et al. (2009) proposes the direct inversion of the system formed by Equations 5 to 7, imposing that $l_{i,kp}$ = 1 and letting the e_{kl}s to be the unknowns. This leads to a system of equations that is ill-conditioned, since it is a discrete form of a variation of the Fredholm integral of the first kind Hansen (1997). In addition, the number of equations and the number of unknowns are not the same, unless KP = KL. As a consequence, the solution of the system of equations can render physically meaningful answers only if regularization methods are applied. One serious limitation of the direct inversion is that it requires the specification of the location of light sources, since there seems to be no clear way to also set their location as unknowns to be determined. Therefore, the obtained results can be among the best for the proposed configuration, but not for all possible configurations.

Optimization

The *IMIbyOPTIM* searches to avoid that trial and error procedure, by considering that the configurations of the light sources are sought to minimize the deviation between the specified and resulting illuminance on the work plane. This approach enables to perform different options of design, by searching light positions, source power or other relevant parameters. The optimization of the accuracy of the solution can be accomplished by requiring that the configurations of the light sources minimize the following objective function Cassol (2009):

$$G = \sqrt{\sum_{kp=1}^{KP} (l_{i,kp} - 1)^2} \quad (9)$$

where KP and KL are respectively the number of work plane elements and light sources of the system. The objective function *G* is composed by a least-square of the deviations between the specified illuminance (in dimensionless form it is equal to unity) and the illuminance on each element kp, that is obtained from a given configuration of light source. Solution was performed by the aid of the generalized extremal optimization (GEO) de Sousa et al. (2003). This algorithm was developed to be easily applicable to a broad class of nonlinear constrained problems.

WORKBENCH DESCRIPTION

The main goal of the present paper is to report the experimental verification of the illuminance uniformity over an indoor work plane, due to the source positioning obtained after the application of *IMIbyOPTIM*. Simulations were performed keeping light sources limited to 32 elements with fixed illuminance power e, giving several configurations of light positioning over the ceiling. The optimized light sources distribution over the ceiling workbench is presented in Figure 2.

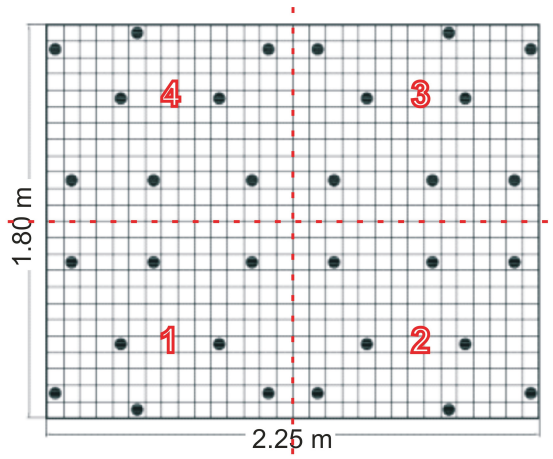

Figure 2: Light sources distribution over the ceiling workbench divided in 4 quarters.

An experimental workbench was then built to reproduce that simulated case, with internal dimensions of 2.25m x 1.80m x 0.45m (length, wide and height). The test enclosure was built with 15 mm thick medium-density fibreboard (MDF). Due to the presence of the illumination sensor in the workbench, the enclosure height had to be increased on 0.14 m, in order to keep the free original height of 0.45m, show in Figure 3.

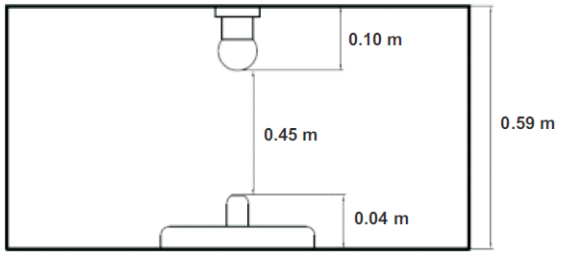

Figure 3: Increase in the enclosure height.

After that adjustment, the work plane is no longer considered the floor of the workbench, but a plane parallel to the floor, situated at an elevation h = 0.04 m. Light sources were also adapted, as there was no power specification on the simulation study. For the sake of safety and convenience, incandescent 15 W bulb lamps were chosen as the light sources. Milky bulb lamps were chosen to reduce the effect of spot light caused by tungsten filament.
The value of the most relevant parameters for both the experimental the simulation study are presented on the next table.

Table 1: Geometrical and radiant parameters of the experiment

PARAMETERS	SIMULATION	WORKBENCH
L	15 m	2.25 m
W	12 m (W/L=0.8)	1.80 m (W/L=0.8)
H	3 m (H/L=0.2)	0.45 m (H/L=0.2)
ρ_{jw}	0.5	0.663
ρ_{jd}	0.1	0.038
ρ_{jl}	0.5	0.663

Geometrical dimensions were reduced by a scale factor of 6.67, keeping the same aspect ratio W/L and H/L, ensuring its dimensional similarity. Although the actual surface reflectivity display differences if compared to the simulated case, they were effectively measured, assuring them to behave as gray, diffuse and opaque surfaces.

EXPERIMENTAL DESCRIPTION

The photovoltaic cell based pyranometer (Apogee model SP-110) was adapted to measure the illuminance field at he work plane. Although designed to measure solar radiation, the pyranometer displayed a good response for visible light from thermal sources, as incandescent bulbs.
Results from IMIbyOPTIM simulations (Cassol, 2009) were reported in respect to a 432 square elements grid, which is a resolution of about 7.5 cm x 7.5 cm, to close to the pyranometer dimensions. Some preliminary results showed that 48 measurement points distributed along the work plane would ensure the experimental verification. Figure 4 depicts that distribution, symmetrically numbered in respect to the 4 quarters of the work plane.
A grid composed by 432 square elements was proposed by the simulation procedure, (Cassol, 2009), and reproduced on the present work. For the experimental setup 12 measurement point were uniformly selected of each quarter part of the work plane, as depicted in Figure 4.

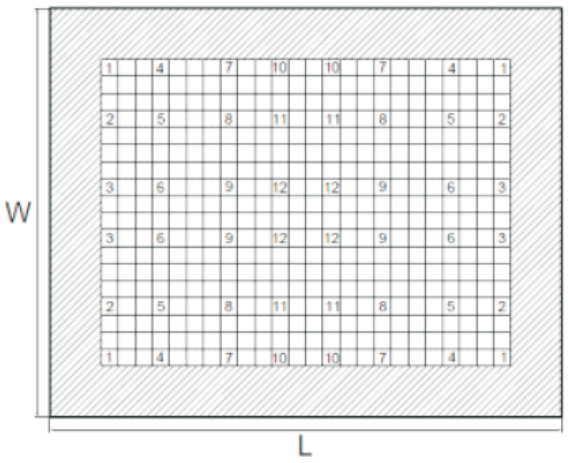

Figure 4: Experimental measurement grid over the work plane.

Table 2: Experimental dimensionless illuminance over the four quarters of the work plane. Positions are relative to the sensor coordinates of Figure 4.

POINT	1-QUAD	2-QUAD	3-QUAD	4-QUAD	POINT AVERAGE
1	1.0149	0.9922	1.0103	0.9854	1.0007
2	0.9945	0.9922	1.0103	0.9967	0.9984
3	0.9899	0.9922	0.9990	1.0013	0.9956
4	1.0035	0.9967	1.0194	1.0058	1.0064
5	1.0058	1.0035	1.0217	0.9990	1.0075
6	1.0103	1.0081	1.0149	1.0035	1.0092
7	0.9741	0.9967	1.0035	0.9786	0.9882
8	0.9832	0.9967	1.0058	0.9922	0.9945
9	0.9945	0.9899	1.0013	0.9945	0.9951
10	0.9922	1.0035	1.0217	1.0126	1.0075
11	0.9809	0.9877	1.0103	1.0081	0.9968
12	0.9945	0.9899	1.0126	1.0126	1.0024
QUARTER AVERAGE	0.9949	0.9958	1.0101	0.9992	**1.0002**
STD DEVIATION	0.0122	0.0064	0.0081	0.0104	0.0065
TARGET RELATIVE BIAS (%)	0.5142	0.4225	1.0900	0.0808	0.0181

Table 3: Comparison between workbench averages and values evaluated for the enclosure (Cassol, 2009).

POINT	POINT AVERAGE	BIAS	ENCLOSURE	BIAS	ERROR
1	1.0007	-0.0007	0.9888	0.0112	1.20
2	0.9984	0.0016	0.9639	0.0361	3.58
3	0.9956	0.0044	0.9861	0.0139	0.96
4	1.0064	-0.0064	0.9957	0.0043	1.07
5	1.0075	-0.0075	0.9992	0.0008	0.83
6	1.0092	-0.0092	1.0179	-0.0179	0.85
7	0.9882	0.0118	0.9964	0.0036	0.82
8	0.9945	0.0055	1.0008	-0.0008	0.63
9	0.9951	0.0049	0.9953	0.0047	0.03
10	1.0075	-0.0075	1.0316	-0.0316	2.34
11	0.9968	0.0032	0.9886	0.0114	0.82
12	1.0024	-0.0024	1.0247	-0.0247	2.18
AVERAGE	1.0002	-0.0002	0.9991	0.0009	0.11

That assembling allowed for the experimental measurement of the illuminance field generated by the 32 light sources, Figure 2, directly by the radiation sensor (pyranometer) on 48 measurement points over the work plane, Figure 4.

RESULTS AND DISCUSSIONS

Sensor output was directly measured in tension (mV), normalized by its average value. Table 2 display the measured results in respect to the four work plane quarters. Table 2 brings in detail all the dimensionless illuminance values measured on the work plane. Values are separated by symmetrical quarters and its mean values, reported on the bottom of the table, indicate that the experimental illuminance field is close to the prescribed unitary dimensionless value. For each of the quarters, the uniformity of the field is once more observed, as the standard deviations represent about one percent of the unitary value. The bias or deviation around the unitary dimensionless target is again assessed at the very end of the table, by the target relative bias, whose values are no bigger than 0.5%.

An auxiliary view of the results is given at the table right hand column. Its values are correspond to the measured average over every symmetric point, numbered identically on Figure 4, and very little difference among then were identified. Finally, the overall experimental dimensionless illuminance average over the work plane, highlighted on bold on the bottom of that same column, shows that the mean value is close to the unitary target, with a standard deviation less than 0.0065.

The dimensionless experimental and simulated illuminances over the entire the work plane are presented on Figure 5 and 6, respectively. The experimental surface allows for concluding that the dimensionless illuminance flux over the work plane is uniform, although some peaks and valleys can be observed. Results confirm the effectiveness of *IMIbyOPTIM* when used for

lighting design for indoors environments. Simulated results for the dimensionless illuminance flux were as good as the experimental ones.

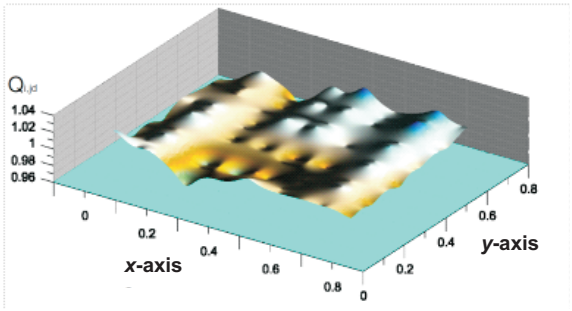

Figure 5: Experimental dimensionless illuminance over the workbench work plane.

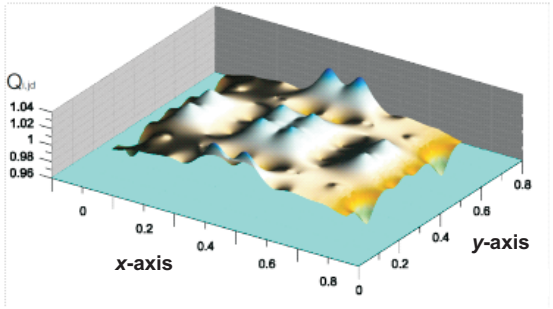

Figure 6: Simulated dimensionless illuminance over the work plane.

Table 2 right hand column is rewritten in Table 3 in order to compare the averages of the measured values to the reference ones. Moreover, it shows the calculated bias and the relative difference between the workbench averages and those obtained by simulation. In regard to the first one, the minimum and maximum bias for the workbench was -0.0092 and 0.0118, respectively. On the other hand, the minimum and maximum bias was -0.0316 and 0.0361. It can be seen that the experimental results are similar to the simulation case. The largest relative difference between the results was 3.58% for point 2, while the lowest was 0.03% for point 9.

CONCLUSION

Experimental results obtained on the workbench indicate that the dimensionless illuminance field is close to the prescribed unitary dimensionless value, the target illuminance. For each of the quarters, the uniformity of the field was once more observed and the target relative bias displayed values no bigger than 0.5%. Moreover, the overall average showed that the mean value was close to the unitary target, with a less than 0.0065 standard deviation. It can be concluded that the experiment was successful, since uniformity in the work plane was achieved. These results demonstrate the effectiveness of the inverse method when used in artificial lighting design. This work appears as the first step in testing the simulated results generated by the *IMIbyOPTIM*. It follows that the subject is far from closed. Rather, there is still much to be done to effectively validate the results produced by simulations. A range of studies and experiments can be carried out accordingly. It is suggested, for example, the improvement of the numerical code to simulate a wider variety of geometries with different surface and radiative proprieties.

NOMENCLATURE

$e_{k\_}$	=	elements dimensionless luminous power
E_{kl}	=	luminous power of the light source element [lx]
$F_{\_,\_}$	=	form factor between surfaces
G	=	objective function
H	=	height of the enclosures $[m]$
H_p	=	dimensionless height of the enclosure (H/L)
kl	=	light source element
kp	=	project surface (work plane) element
kw	=	wall element
KL	=	total number of lamps elements
KP	=	total number of project surfaces (work plane)
KW	=	total number of walls
$l_{i,k\_}$	=	dimensionless incident illuminance on element $k\_$
$l_{0,k\_}$	=	dimensionless outgoing illuminance on element $k\_$
L	=	length of the enclosures $[m]$
L_p	=	dimensionless length of the enclosure (L/L)
$L_{i,spf}$	=	specified luminous flux on the work plane $[lx]$
$L_{i,k\_}$	=	incident illuminance on element $k\_$ $[lx]$
$L_{0,k\_}$	=	outgoing illuminance on element $k\_$ $[lx]$
W	=	width of the enclosures $[m]$
W_p	=	dimensionless width of the enclosure (W/L)
$\rho_{j\_}$	=	surfaces hemispherical reflectivity

ACKNOWLEDGEMENT

Jenisch Rodrigues acknowledges CAPES (PNPD 02784/09-2) for her post doctoral fellowship at UFRGS, Smith-Schneider and França acknowledges CNPq for their research grants PQ 308756/2009-6 and PQ 304535/2007-9. All authors thank the mechanical technician João Batista da Rosa for support and technical assistance in building the experimental workbench.

REFERENCES

Cassol, F. 2009. Aplicação da análise inversa via otimização extrema generalizada em projetos de iluminação. Master's thesis, PROMEC/UFRGS - Programa de Pós-Graduação em Engenharia Mecânica, Porto Alegre, RS, Brazil.

Cavichioli, J., Ruggiero, C., Volpe, C., Paulo, E., Fagundes, J., and Kasai, F. 2006. Florescimento e frutificação do maracujeiro-amarelo submetido à iluminação artificial, irrigação e sombreamento. *Revista Brasileira de Fruticultura*, 28(1):92–96.

Daun, K., França, F., Larsen, M., Leduc, G., and Howell, J. 2006. Comparison of methods for inverse design of radiant enclosures. *Journal of Heat Transfer*, 128:269–282.

de Sousa, F., Ramos, F., Paglione, P., and Girardi, R. 2003. New stochastic algorithm for design optimization. *AAIA Journal*, 41(9):1808–1818.

EEE/SA 2012. *Product Catalogue*. Empresa de Equipamento Elétrico SA, Lisboa. url: http//www.eee.pt.

Ertürk, H., Ezekoye, O., and Howell, J. 2002. Comparison of three regularized solution techniques in a three-dimensional inverse radiation problem. *Journal of Quantitative Spectroscopy and Radiative Transfer*, 73:307–316.

Fontana, D., Schneider, P., and França, F. 2004. Projeto inverso aplicado ao dimensionamento de sistemas de iluminação de ambientes. In *Proceedings of XXV Iberian Latin American Congress in Computacional Methods in Engineering*.

França, F. and Howell, J. 2006. Transient inverse design of radiative enclosures for thermal processing of materials. *Inverse Problems in Science and Engineering*, 14:423–436.

França, F., Howell, J., Ezekoye, O., and Morales, J. 2002. Inverse design to thermal systems. *Advances in Heat Transfer*, 36:1–110.

Hansen, P. 1997. *Rank-Deficient and discrete ill-posed problems*. SIAM, Philadelphia, PA.

Harrison, W. and Anderson, E. 1916. Illumination efficiences as determinated in an experimental room. *Trans. Ilum. Eng. Soc.*, 11:67–91.

Harrison, W. and Anderson, E. 1920. Coeficients of utilization. *Trans. Ilum. Eng. Soc.*, 15:97–123.

Hottel, H. and Sarofim, A. 1967. *Radiaton Transfer*. McGraw-Hill New York.

IESNA 2000. *The IESNA Lighting Handbook: reference and application*. Illumination Engineering Society of North America, New York, 9 edition.

Jordan, R. and Tavares, M. 2005. Análise de diferentes sistemas de iluminação para aviários de produção de ovos férteis. *Revista Brasileira de Engenharia Agrícola e Ambiental*, 9(3):420–423.

Moon, P. 1941. Interreflections in rooms. *J. Optical Soc. Am.*, 20:374–382.

Moon, P. and Spencer, D. 1946a. Light design by the interrefletion method. *J. Franklin Inst.*, 242:465–501.

Moon, P. and Spencer, D. 1946b. Light distribution in rooms. *J. Franklin Inst.*, 242:111–141.

Schneider, P. and França, F. 2008. Inverse design analysis applied to an illumination design. *Engenharia Térmica*, 6(1):26–40.

Schneider, P., Mossi, A., França, F., de Sousa, F., and da Silva Neto, A. 2009. Application of inverse analysis to illumination design. *Inv. Probl. in Sci. and Eng.*, 17(16):737–753.

Seewald, A. 2006. Análise inversa em cavidades radiantes com superfícies não-cinzas uma abordagem para projetos de iluminação. Master's thesis, PROMEC/UFRGS - Programa de Pós-Graduação em Engenharia Mecânica, Porto Alegre, RS, Brazil.

Siegel, R. and Howell, J. 2002. *Thermal Radiaton and Heat Transfer*. Hemisphere Publishing Corporation - Washington.